Unconventional mechanism of virtual-state population through dissipation

Alejandro Vivas-Viaña,[1] Alejandro González-Tudela,[2] and Carlos Sánchez Muñoz[1,*]
[1]*Departamento de Física Teórica de la Materia Condensada and Condensed Matter Physics Center (IFIMAC), Universidad Autónoma de Madrid, 28049 Madrid, Spain*
[2]*Institute of Fundamental Physics IFF-CSIC, Calle Serrano 113b, 28006 Madrid, Spain*

(Received 4 March 2022; accepted 29 June 2022; published 22 July 2022)

Virtual states are a central concept in quantum mechanics. By definition, the probability of finding a quantum system in a virtual state should be vanishingly small at all times. In contrast to this notion, we report a phenomenon occurring in open quantum systems by which virtual states can acquire a sizable population in the long-time limit, even if they are not directly coupled to any dissipative channel. This means that the situation in which the virtual state remains unpopulated can be metastable. We describe this effect by introducing a two-step adiabatic elimination method, which we termed hierarchical adiabatic elimination, that allows one to obtain analytical expressions of the timescale of metastability in general open quantum systems. We show how these results can be relevant for practical questions such as the generation of stable and metastable entangled states in dissipative systems of interacting qubits.

DOI: 10.1103/PhysRevA.106.012217

I. INTRODUCTION

The concept of virtual state in quantum mechanics is of paramount importance, e.g., in the context of virtual transitions between coherently unconnected states [1–3] or in the description of scattering processes in quantum field theory where interactions are mediated by virtual particles [4]. In situations in which strongly off-resonant "virtual" states mediate interactions between quasiresonant "real" states, an adiabatic elimination over the fast degrees of freedom—the virtual ones—allows one to reduce the dimensionality of the problem and obtain an effective description of the slow degrees of freedom, i.e., the real states. This technique of adiabatic elimination, which can be formulated in several alternative ways—e.g., the Schrieffer-Wolff transformation [2]—is ubiquitous in the description and design of quantum phenomena, e.g., quantum optical applications in atomic physics [5–15] or exotic dynamics in the ultrastrong coupling regime of cavity QED [16–18]. A significant effort has been made to establish the mathematical foundations of this technique [19–21] and its extension to dissipative contexts for its application in open quantum systems [22–25].

The notion of virtual states can be unambiguously invoked in a Hamiltonian context whenever the eigenenergies of a bare Hamiltonian $\hat{H}_0$ are grouped in clusters that are energetically well separated from each other [2]. If we denote these levels as $E_{i,\alpha}$, with the index i labeling states within a cluster, and α labeling the different clusters, such a condition reads

$$|E_{i,\alpha} - E_{j,\alpha}| \ll |E_{i,\alpha} - E_{j,\beta}| \quad (\alpha \neq \beta). \tag{1}$$

Given a cluster α, the eigenstates $|i,\alpha\rangle$ conforming it span a Hilbert subspace that we denote $\mathcal{H}_\alpha$. Let us now consider that the Hamiltonian contains a small perturbation term $\hat{V}$, yielding a coupling between manifolds that is much smaller than their energy difference,

$$|\langle i,\alpha|\hat{V}|j,\beta\rangle| \ll |E_{i,\alpha} - E_{j,\beta}|. \tag{2}$$

In this case, the resulting energy eigenstates remain clustered in the same manifold structure, and second-order perturbation theory allows one to describe the dynamics in terms of an effective block-diagonal Hamiltonian that does not couple different manifolds. This means that the evolution of any initial state belonging to a given subspace, which we denote the "real" subspace $\mathcal{H}_R$, evolves effectively constrained within that subspace. The remaining manifolds, which are strongly out of resonance, span the subspace of "virtual" states $\mathcal{H}_V$, which are effectively unpopulated at all times—hence their name—but contribute to the dynamics in $\mathcal{H}_R$ yielding effective energy shifts and interactions among the "real" states. This establishes the definition of a virtual state that we consider here: a state very detuned from the subspace where the dynamics is taking place and weakly coupled to it, so that its only effect is to provide effective energy shifts and interactions, without even becoming populated.

In this work, we show that the intuitive notion that a virtual state remains unpopulated can be false in the presence of dissipation even if the virtual state is not directly coupled to any dissipative channel. We unveil an unconventional mechanism by which, in the long-time limit, virtual states acquire a sizable occupation probability, comparable to that of the real states, even when dissipative processes only take place within $\mathcal{H}_R$. These findings can be relevant for the understanding and design of dissipative processes for quantum state preparation or engineered interactions [26–35].

To study this phenomenon, in Sec. II we start discussing what is arguably the simplest scenario that can be described

*carlos.sanchezmunnoz@uam.es

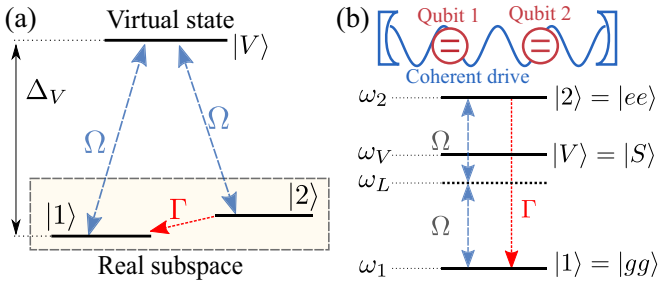

FIG. 1. (a) Scheme of the system: two quasiresonant "real" quantum states, interacting via a third, strongly off-resonant virtual state. There is spontaneous decay between the real states. (b) The system in (a) can describe two interacting two-level systems under coherent driving at the two-photon resonance, in the rotating frame of the drive. Decay between real states can be engineered with a cavity.

in terms of virtual states [see Fig. 1(a)]: two quasiresonant real states, effectively interacting through the mediation of a third, strongly off-resonant virtual state. Crucially, we enable a spontaneous decay between the real states, which can be provided, for instance, by the coupling to a surrounding environment in a Markovian regime. We show that, contrary to the familiar intuition, the situation in which the virtual state remains "virtual"—i.e., unpopulated—is, in this case, only metastable [36,37], and, in the long-time limit, the system eventually relaxes to a stationary state where the virtual state has a sizable population. This process of *de-virtualization* occurs through an unconventional mechanism of population enabled by dissipation. In Sec. III, we introduce a technique of hierarchical adiabatic elimination (HAE) to obtain analytical approximations of the time-dependent elements of the system density matrix and expressions for the characteristic metastability timescales. In Sec. IV, we provide essential intuition about the underlying mechanism of population through the analysis of quantum trajectories [38–40], showing that the virtual state gets populated due to the non-Hermitian evolution taking place between quantum jumps. Finally, in Sec. V we discuss the generality of the HAE technique, showing how it can be used to describe metastable dynamics in different systems involving two interacting qubits, where the phenomenon reported has strong implications for the generation of stable and metastable entanglement via dissipation [41,42].

II. MODEL

The first model we study consists of a three-level system configuration, sketched in Fig. 1(a). The Hilbert space spans a basis $\{|1\rangle, |2\rangle, |V\rangle\}$, where the states $|1\rangle$ and $|2\rangle$ represent two real states, and $|V\rangle$ will play the role of a virtual state, being strongly detuned from $|1\rangle$ and $|2\rangle$. We define lowering operators as $\hat{\sigma}_{i,j} \equiv |i\rangle\langle j|$ $(i, j = 1, 2, V)$. The real states are coupled to $|V\rangle$ with a coupling rate Ω, and there is an irreversible decay process within the real subspace, with state $|2\rangle$ decaying towards $|1\rangle$ with a decay rate Γ. This specific Λ model could be motivated, for instance, by the description of a quantum-optical system consisting of two interacting qubits coherently excited at the two-photon resonance with a Rabi frequency Ω [43–46], where the ground state $|gg\rangle$ corresponds to the real state $|1\rangle$, the doubly excited state $|ee\rangle$ is the excited real state $|2\rangle$, and the symmetric single-excitation state $|S\rangle = \frac{1}{\sqrt{2}}(|eg\rangle + |ge\rangle)$—detuned from the two-photon transition energy due to the interaction between qubits—corresponds to the virtual state $|V\rangle$. The two-photon decay channel can be enabled, for instance, by a cavity in resonance with the two-photon transition [47,48]. A change to the rotating frame of the drive would directly yield the configuration shown in Fig. 1(a). The resulting time-independent Hamiltonian is $\hat{H} = \hat{H}_0 + \hat{H}_d$, where $\hat{H}_0$ is the bare Hamiltonian ($\hbar = 1$),

$$\hat{H}_0 = \Delta_1|1\rangle\langle 1| + \Delta_2|2\rangle\langle 2| + \Delta_V|V\rangle\langle V|, \tag{3}$$

and $\hat{H}_d$ is the Hamiltonian of the driving/coupling term,

$$\hat{H}_d = \Omega(\hat{\sigma}_{1,V} + \hat{\sigma}_{2,V} + \text{H.c.}), \tag{4}$$

where Δ_i $(i = 1, 2, V)$ denote the free-energy parameters, where we will assume that $\Delta_V \gg \Delta_2, \Delta_1, \Omega$ and $\Delta_2 \approx \Delta_1 \approx 0$. We assume that the evolution of the system is governed by a quantum master equation [49],

$$\frac{d\hat{\rho}}{dt} = -i[\hat{H}, \hat{\rho}] + \frac{\Gamma}{2}\mathcal{L}_{\hat{\sigma}_{21}}[\hat{\rho}] + \frac{\Gamma_V}{2}\mathcal{L}_{\hat{\sigma}_{1V}}[\hat{\rho}], \tag{5}$$

where the Lindblad term $\mathcal{L}_{\hat{O}} \equiv 2\hat{O}\hat{\rho}\hat{O}^\dagger - \{\hat{O}^\dagger\hat{O}, \hat{\rho}\}$ describes processes of spontaneous decay. Unless stated otherwise, we will consider $\Gamma_V = 0$, i.e., we assume there is only one process of spontaneous decay, from $|2\rangle$ to $|1\rangle$ (the case $\Gamma_V \neq 0$ will be considered later only for comparison). The dynamics of the system can be studied straightforwardly by numerically solving Eq. (5). Figure 2(a) shows the occupation probability of the excited state, $\rho_{2,2} \equiv \langle 2|\hat{\rho}|2\rangle$, and the virtual state, $\rho_{V,V} \equiv \langle V|\hat{\rho}|V\rangle$, versus time. One can clearly appreciate the existence of two distinct relaxation timescales. Within the first relaxation timescale ($t \sim 1/\Gamma$), the system behaves according to the standard intuition regarding virtual states: $|V\rangle$ remains unpopulated, mediating the interaction between $|1\rangle$ and $|2\rangle$, which gives rise to coherent Rabi oscillations between these two states with a two-photon Rabi frequency $\Omega_{2p} = \Omega^2/\Delta_V$, damped by spontaneous emission of rate Γ into a stationary state. This situation can be described simply in terms of a coherently driven two-level system spanned by $|1\rangle$ and $|2\rangle$. This stationary regime is, however, metastable, and in a much longer timescale, which for this particular choice or parameters is $t \sim 10^4/\Gamma$, $\rho_{V,V}$ develops a population comparable to $\rho_{2,2}$. Clear evidence of this metastable behavior in open quantum systems can be found in the spectrum of eigenvalues of the Liouvillian superoperator $\mathcal{L}$ [36,37]. All of these eigenvalues $\{\lambda_k, k = 1, 2, \ldots\}$—ordered here by their real values, so that $\text{Re}(\lambda_k) \geqslant \text{Re}(\lambda_{k+1})$—have a negative real part, and the eigenvalue with the largest real part is necessarily equal to zero, $\lambda_1 = 0$, its corresponding eigenstate being the steady state of the system. The second largest real value of the Liouvillian spectrum, $\text{Re}(\lambda_2)$, is the Liouvillian gap [50], and it gives the relaxation time necessary to reach the steady state, $\tau_2 = 1/|\text{Re}(\lambda_2)|$. Metastability results when λ_2 is well separated from the rest of eigenvalues by a second gap, so that $\text{Re}(\lambda_3) \ll \text{Re}(\lambda_2)$ [36] (here, we assume for simplicity that, as in the case of our model, there is only one metastable state, rather than a manifold). Then, the system relaxes to a metastable state in a timescale $\tau_3 = 1/|\text{Re}(\lambda_3)|$,

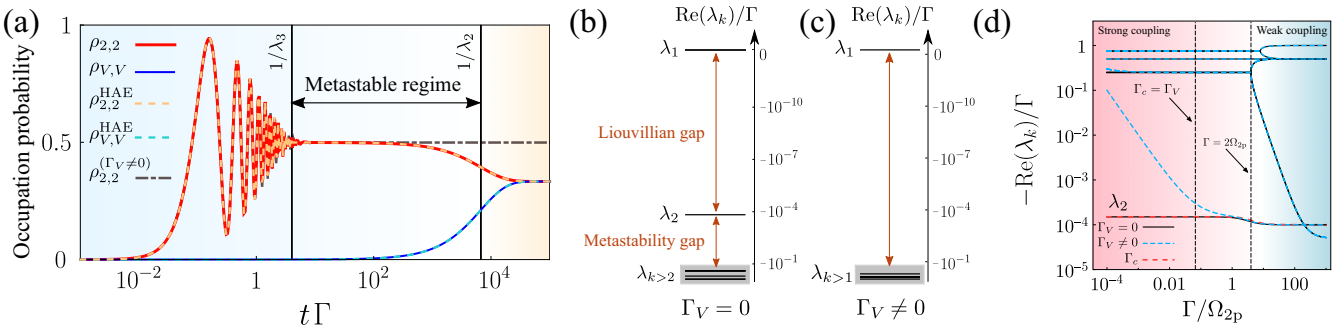

FIG. 2. (a) Dynamics of the excited real state and the virtual state. Solid lines are numerical calculations, dashed lines are analytical predictions from the hierarchical adiabatic elimination. The dot-dashed line represents a case in which $\Gamma_V \neq 0$, showing the stabilization of the metastable state. (b) Liouvillian spectrum, featuring the defining characteristic of metastability in open quantum systems: a metastability gap between λ_2 and $\lambda_{k>2}$. (c) Same as in (b), with $\Gamma_V = \Gamma$. In this system, metastability is no longer present. (d) Liouvillian eigenvalues vs Γ for $\Gamma_V = 0$ (solid, black) and $\Gamma_V = 10^{-5}\Omega_{2p}$. Our analytical prediction for the value of the Liouvillian gap λ_2 for $\Gamma_V =$ is shown by a dashed red line. If $\Gamma_V \neq 0$, it is seen that metastability disappears when $\Gamma_c < \Gamma_V$. Parameters: $\Omega/\Delta_V = 0.01$; in (a)–(c), $\Gamma/\Delta_V = 10^{-5}$. Γ_V is zero unless indicated otherwise, in which case $\Gamma_V = \Gamma$.

which will eventually evolve into the actual steady state in a time $\tau_2 \gg \tau_3$. The system we consider here exhibits precisely this clustering of eigenvalues characteristic of metastability, as can be seen in Fig. 2(b) where we confirm that $\tau_3 \sim 1/\Gamma$ and $\tau_2 \sim 10^4/\Gamma$. The steady state value of the virtual-state occupation probability can be computed analytically, yielding

$$\rho^{\rm ss}_{V,V} = \frac{\Omega^2(\Gamma^2 + 4\Omega^2)}{2\Omega^2(\Gamma^2 + 6\Omega^2) + \Gamma^2\Delta_V^2}. \tag{6}$$

In the limit $\Omega^2 \gg \Gamma\Delta_V$, this expression indeed yields a sizable population $\rho^{\rm ss}_{V,V} \approx 1/3$, clearly establishing that the virtual state will get populated in the long-time limit.

III. HIERARCHICAL ADIABATIC ELIMINATION

To have an estimate of the survival time of the metastable state, it would be desirable to obtain an analytical expression of λ_2. A direct analytical solution for the time evolution of the density matrix through the diagonalization of $\mathcal{L}$ is not readily available. Nevertheless, it is clear from our previous discussion that there is a hierarchy of timescales, which suggests that a series of adiabatic elimination techniques could be applied. (i) The shortest timescale is clearly governed by Hamiltonian dynamics, evidenced by a fast oscillatory evolution of the density matrix elements. This oscillatory dynamics stabilizes into a steady state in a timescale of the order $\tau_3 \sim 1/\Gamma$. In these timescales, the population of $|V\rangle$ plays the role of a fast variable: $|V\rangle$ mediates effective interactions within the real subspace, i.e., it plays the role of a virtual state that can be eliminated within a purely Hamiltonian evolution. This is the first adiabatic elimination that we will perform. (ii) The longest timescale is characterized by a very slow evolution of $|V\rangle$. In this long timescale, the relaxation of the real variables in a time $1/\Gamma$ occurs almost instantaneously, meaning that one can treat the real variables as the *fast* variables in a dissipative sense, i.e., they relax quickly into a time-dependent quasisteady state that follows the slow evolution of $\rho_{V,V}$. This can be described in terms of a second adiabatic elimination. Note that a direct application of standard adiabatic elimination techniques in a dissipative context, e.g., the projection-operator method [25,51], would directly eliminate the virtual subspace, and thus it would fail to capture the mechanism that populates this state in the long-time limit. We present instead a two-step method, which we label hierarchical adiabatic elimination (HAE).

A. First adiabatic elimination

Our starting point is the set of differential equations describing the evolution of the elements of the total density matrix, obtained from Eq. (5) as

$$\dot\rho_{V,V} = 2\Omega\,\mathrm{Im}[\rho_{1,V} - \rho_{V,2}], \tag{7a}$$
$$\dot\rho_{2,2} = -\Gamma\rho_{2,2} + 2\Omega\,\mathrm{Im}[\rho_{V,2}], \tag{7b}$$
$$\dot\rho_{1,V} = i\Delta_V\rho_{1,V} + i\Omega[1 + \rho_{1,2} - 2\rho_{V,V} - \rho_{2,2}], \tag{7c}$$
$$\dot\rho_{1,2} = -(\Gamma/2)\rho_{1,2} + i\Omega[\rho_{1,V} - \rho_{V,2}], \tag{7d}$$
$$\dot\rho_{V,2} = -(i\Delta_V + \Gamma/2)\rho_{V,2} - i\Omega[\rho_{1,2} + \rho_{2,2} - \rho_{V,V}]. \tag{7e}$$

Based on the assumption that $|\Delta_V - \Delta_i| \gg |\Omega|$ $(i \in \{1, 2\})$, we perform an adiabatic elimination consisting in setting $\dot\rho_{1,V} = \dot\rho_{V,2} = 0$. In the limit $\Delta_V \gg \Gamma$, the resulting effective equations that govern the dynamics of the real subspace become

$$\dot\rho_{2,2} \approx -\Gamma\rho_{2,2} - 2\Omega_{2p}\,\mathrm{Im}[\rho_{1,2}] + \frac{\Gamma\,\Omega_{2p}}{\Delta_V}\rho_{V,V}, \tag{8a}$$
$$\dot\rho_{1,2} \approx -\Gamma/2\,\rho_{1,2} + i\Omega_{2p}(2\rho_{2,2} + \rho_{V,V} - 1), \tag{8b}$$

where we defined a two-photon Rabi frequency, $\Omega_{2p} \equiv \Omega^2/\Delta_V$. These equations can be solved considering $\rho_{V,V}$ as a time-independent parameter with a fixed value (i.e., $\dot\rho_{V,V} = 0$). A natural choice would be to set $\rho_{V,V} = 0$. In that case, Eqs. (8a) and (8b) simply describe the dynamics of two resonant levels coupled via a second-order process with a Rabi frequency of Ω_{2p} with a standard decay, e.g., the regime of coherent two-photon driving of the transition $|gg\rangle \leftrightarrow |ee\rangle$ in the case of a two-atom system depicted in Fig. 1(b). Such a two-level system dynamics describes accurately the short-timescale oscillatory dynamics of Fig. 2(a), where the initial state was set to be $|1\rangle$. From now on, we focus on the

strong-driving limit $\Gamma \lesssim \Omega_{2p}$; otherwise, the system is overdamped and will basically remain in the ground state $|1\rangle$.

B. Second adiabatic elimination

While the usual approach when eliminating a virtual state is to indeed assume $\rho_{V,V} = 0$ for all times, we have already seen that this approach is eventually bound to fail, since $\rho_{V,V}$ develops a sizable population within a characteristic timescale $\tau_2 \gg 1/\Gamma$, which, crucially, is orders of magnitude longer than the relaxation time of Eqs. (8a) and (8b). This suggests that we can make a second adiabatic elimination based on this separation of timescales. From the first adiabatic elimination conditions ($\dot{\rho}_{V,i} = 0$) and Eq. (7a), we can obtain a differential equation for $\rho_{V,V}$ that is a function of itself and the real-subspace elements, i.e., $\dot{\rho}_{V,V}(t) = f[\rho_{V,V}(t); \rho_{1,2}(t); \rho_{2,2}(t)]$ (see Appendix A 2 for a full expression). The second adiabatic elimination consists in substituting $\rho_{1,2}(t)$ and $\rho_{2,2}(t)$ in that equation by their corresponding steady-state solutions of Eqs. (8a) and (8b), $\rho^{ss}_{1,2}(\rho_{V,V}(t))$ and $\rho^{ss}_{2,2}(\rho_{V,V}(t))$, which are obtained for a given $\rho_{V,V} = \rho_{V,V}(t)$. This yields a dynamical equation that only depends on $\rho_{V,V}(t)$, i.e.,

$$\dot{\rho}_{V,V}(t) = f\left[\rho_{V,V}(t); \rho^{ss}_{1,2}(\rho_{V,V}(t)); \rho^{ss}_{2,2}(\rho_{V,V}(t))\right]. \quad (9)$$

In this approximation, $\rho_{2,2}$ and $\rho_{1,2}$ act as fast variables that relax into a time-dependent stationary state that follows the slow evolution of $\rho_{V,V}$. Solving this differential equation, one obtains $\rho_{V,V}(t) \approx \rho^{ss}_{V,V}(1 - e^{-\Gamma_c t})$, where we have defined the relaxation rate

$$\Gamma_c \approx \frac{3\Gamma\Omega^2}{2\Delta_V^2}, \quad (10)$$

obtained under the assumption $\Omega_{2p} \gg \Gamma$ (a full, more cumbersome expression that does not require that assumption is provided in the Appendix A 2). Equation (10) is the desired expression that gives us the survival time of the metastable regime, and thus it must correspond to the Liouvillian gap, $\Gamma_c = |\mathrm{Re}(\lambda_2)|$. We have checked that this is indeed the case in Fig. 2(d), which depicts the spectrum of eigenvalues of $\mathcal{L}$ as a function of Γ, showing a perfect match between our analytical expression of Γ_c and λ_2. A similar comparison versus both Γ and Ω is shown in Appendix B. We also note the perfect matching between exact results and analytical solutions of the dynamics in Fig. 2(a), where we used the full expressions in Appendix A 3. Further comparisons between exact results and analytical expressions, including approximated ones such as Eq. (10), are shown in Appendix B.

IV. MECHANISM OF POPULATION

We will now provide some insights into the dissipative mechanism that populates the virtual state. To do so, we perform an analysis from the perspective of quantum trajectories using the method of quantum jumps [38–40]. Inspection of individual trajectories—see, e.g., the example of Fig. 3(a)—reveals that the virtual state gets populated through non-Hermitian evolution between quantum jumps—the effect of a jump is, in fact, to strongly decrease the population of the virtual state. This can be understood if one considers the information about the system leaked to the environment during

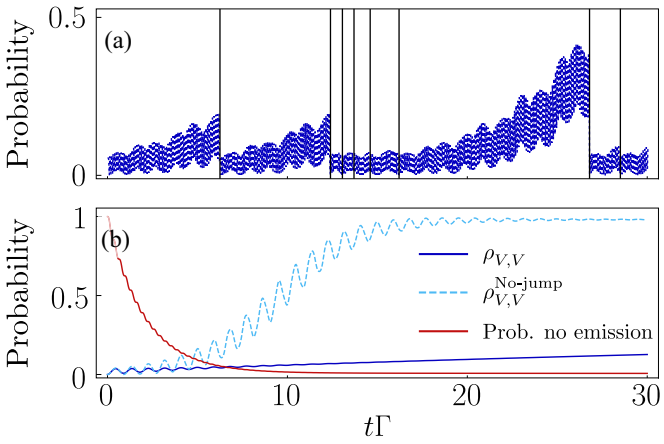

FIG. 3. (a) Population of the virtual state through non-Hermitian evolution between quantum jumps. (b) Conditional evolution when no jumps take place. Red line: probability of no jump. Blue dashed line: population of the virtual state conditioned to no jumps, showing that, in this case, it reaches its maximum possible value. Blue straight line: population of the virtual state for the general evolution. Parameters: $\Omega/\Delta_V = 0.1$, $\Gamma/\Delta_V = 10^{-3}$, $\Delta_2 = \Delta_1 = 0$.

a time interval with no jumps [52]. When no jump occurs, the system is logically more likely to be in a state that cannot emit, i.e., either $|1\rangle$ or $|V\rangle$. However, since $|1\rangle$ is resonantly coupled to $|2\rangle$ to second order in perturbation theory, a system in $|1\rangle$ will eventually evolve into $|2\rangle$ and lead to a jump. In other words, as a period without a jump becomes longer, $|V\rangle$ becomes the most likely state, and the system is updated accordingly, increasing its population. This purely dissipative mechanism will slowly accumulate over time, explaining the population buildup of the virtual state in our system. This intuition is further confirmed by computing a conditional density matrix for the particular trajectory in which no jumps occur at all; see Fig. 3(b). In this particular scenario (whose probability decreases over time, as is expected), the population of the virtual state saturates to its maximum possible value, confirming that the non-Hermitian evolution in the absence of jumps is responsible for the population of the virtual state.

This mechanism would be completely disrupted if there were additional dissipative channels involving the virtual state. We can consider this situation by setting $\Gamma_V \neq 0$ in Eq. (5), thus including a channel of spontaneous emission from the virtual state to the ground state. The ratio between decay rates, Γ_V/Γ_c, will determine whether virtual-state population occurs or not. When $\Gamma_V \gtrsim \Gamma_c$, dissipation from $|V\rangle$ outcompetes the mechanism of population, and one recovers the simple dynamics in terms of a driven two-level system, as can be seen in Fig. 2(a). Consistent with this, there is no longer a Liouvillian eigenvalue corresponding to a metastable state– - as shown in Figs. 2(c) and 2(d)—as Γ_V becomes comparable to Γ_c, λ_2 is pulled towards values $\sim\Gamma$, and the metastability gap disappears. The calculation of Γ_c thus allows us to establish a minimum value for Γ_V to guarantee that the unconventional population of virtual states does not take place. This is relevant for situations in which this effect is undesirable, as can be seen in the case of protocols of dissipative cooling into entangled states [29–33].

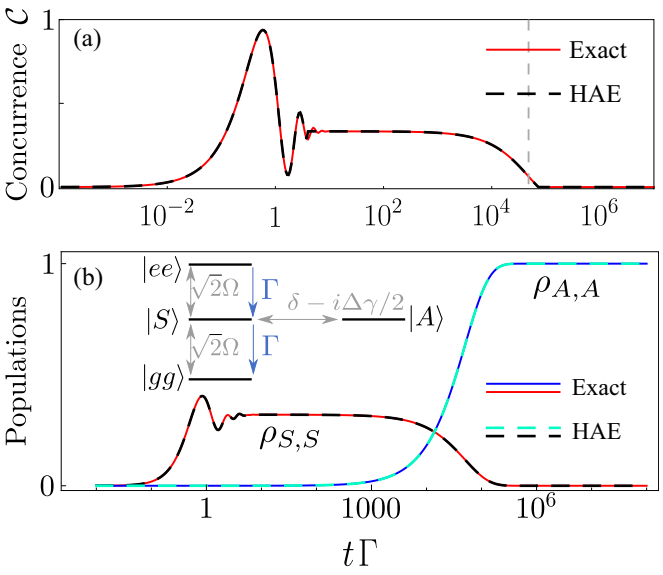

FIG. 4. Entanglement formation in systems of two coupled qubits. (a) Formation of metastable entangled state in the system sketched in Fig. 1(b), surviving for a time $\tau_2 \sim 1/\Gamma_c$. Parameters: $\Gamma/\Delta_V = 10^{-5}$, $\Delta_2/\Delta_V = 0$. (b) Stabilization of the entangled antisymmetric state in the two-qubit system sketched in the inset. The evolution is perfectly described by the HAE. Parameters: $\Omega/\Gamma = 1$, $\delta/\Gamma = 0.01$, $\Delta\gamma/\Gamma = 0.01$.

V. GENERALITY OF THE HAE AND ITS IMPLICATIONS FOR ENTANGLEMENT GENERATION

The HAE method introduced in this work can be a valuable tool to obtain analytical insights about metastable dynamics in open quantum systems. This can have strong implications for quantum technological applications such as the generation of entanglement in dissipative quantum systems. To illustrate this, we now apply the HAE to describe entanglement generation in two different systems displaying metastability.

First, we consider entanglement generation in the system of two interacting qubits already described in Fig. 1(b), which, as noted before, maps into the three-level model discussed so far in this text, assuming that the occupation of the antisymmetric state $|A\rangle \propto (|eg\rangle - |eg\rangle)$ is completely decoupled from the dynamics and remains equal to zero. This map between models allows us to use the density matrix elements estimated with the HAE—cf. Fig. 2(a)—to compute the concurrence and quantify the degree of entanglement between the two qubits [53–56]. The results are shown in Fig. 4(a), evidencing the formation and stabilization of entanglement at short timescales $t \sim 1/\Gamma$, due to the coherence built between the states $|ee\rangle$ and $|gg\rangle$ via the two-photon drive. Notably, this entanglement is long-lived, but metastable, and its survival time is given by $1/\Gamma_c$, i.e., the relaxation rate obtained in Eq. (10) via the HAE. The unconventional population of the virtual state $|S\rangle$ thus destroys entanglement in the long-time limit.

Next, we consider another two-qubit system, sketched in the inset of Fig. 4(b). In this case, qubits experience collective decay with rate Γ, inducing transitions $|ee\rangle \to |S\rangle$ and $|S\rangle \to |gg\rangle$. Furthermore, each qubit is driven with the same Rabi frequency Ω, but each of them is detuned from the drive frequency by an absolute value δ with opposite sign. This system, which was introduced in Refs. [41,42] in the context of chiral waveguides, is described by the Hamiltonian

$$\hat{H} = \sqrt{2}\Omega(|S\rangle\langle gg| + |ee\rangle\langle S|) + (\delta - i\Delta\gamma/2)|A\rangle\langle S| + \text{H.c.}, \tag{11}$$

with $\Gamma = 2(\gamma_R + \gamma_L)$ and $\Delta\gamma \equiv \gamma_R - \gamma_L$, where γ_R and γ_L describe decay into right and left propagating modes, respectively. The corresponding decay channels are sketched in Fig. 4(b); we observe that the state $|A\rangle$ is not coupled to any dissipative channel. This configuration was shown to stabilize in the long-time limit to the fully entangled dark state $|A\rangle$ provided $\Omega \gg \Delta\gamma, \delta$, as we show explicitly in Fig. 4(b). The application of HAE to describe this system follows exactly the same reasoning detailed in Sec. III, with $|A\rangle$ playing the role of the "virtual" state that gets populated over time. Indeed, one can observe that, if one diagonalizes the driving term proportional to Ω in Eq. (11), only two of the three resulting eigenstates are coherently coupled to $|A\rangle$, and both are detuned from it by values $\pm 2\sqrt{2}\Omega$, so that the condition $\Omega \gg \Delta\gamma, \delta$ implies that, at a Hamiltonian level, $|A\rangle$ is expected to play the role of a virtual state. The mechanism of unconventional population of a virtual state is therefore responsible for the formation of entanglement in the long-time limit.

Applying the technique of HAE, we are able to establish the timescale of formation of the entangled state, which is given by

$$\tau \approx \frac{24\Omega^2}{\Gamma(4\delta^2 + \Delta\gamma^2)}. \tag{12}$$

The analytical results obtained from the HAE method match perfectly the exact calculations, as shown in Fig. 4(b). In the limit $(\delta, \Delta\gamma) \to 0$ we find $\tau \to \infty$, meaning that the metastable state becomes the steady state, as reported, e.g., in Ref. [57].

VI. CONCLUSION

We have shown that, in open quantum systems, off-resonant virtual states can get populated in the long-time limit even if they are not connected to any dissipative channel, meaning that the regime where the virtual state is not populated is metastable. We introduce a method of hierarchical adiabatic elimination that approximates the dynamics and provides analytical expressions of the lifetime of the metastable state. Our method can be applied in a variety of metastable open quantum systems to obtain valuable insights into questions such as the dissipative stabilization of entangled states.

ACKNOWLEDGMENTS

The authors are thankful to C. Navarrete-Benlloch for insightful discussions and D. Porras for a critical reading of the manuscript. C.S.M. acknowledges that the project that gave rise to these results received the support of a fellowship from la Caixa Foundation (ID 100010434), from the European Union's Horizon 2020 Research and Innovation Programme under the Marie Sklodowska-Curie Grant Agreement No. 847648, with fellowship code LCF/BQ/PI20/11760026. A.G.T. acknowledges support from CSIC Research Platform

on Quantum Technologies PTI-001 and from Spanish project PGC2018-094792-B-100(MCIU/AEI/FEDER, EU). All authors acknowledge financial support from Proyecto Sinérgico CAM 2020 Y2020/TCS-6545 (NanoQuCo-CM).

APPENDIX A: FURTHER DETAILS ON THE HIERARCHICAL ADIABATIC ELIMINATION

Here, we elaborate on all the steps involved in the hierarchical adiabatic elimination technique. Let us recall that, as an example, we consider a Hilbert space of three states, $\mathcal{H} = \{|1\rangle, |2\rangle, |V\rangle\}$. Here, $|1\rangle$ and $|2\rangle$ represent the "real" states, and $|V\rangle$ is an off-resonant state that plays the role of a virtual state that mediates the interactions between $|1\rangle$ and $|2\rangle$. The evolution of the elements of the density matrix are given by Eq. (7a)–(7e).

1. First adiabatic elimination

The first stage of the dynamics can be completely described within the real Hilbert subspace, $\mathcal{H}_R = \{|1\rangle, |2\rangle\}$, after an adiabatic elimination of the virtual state. More specifically, this adiabatic elimination consists in setting $\dot{\rho}_{1,V} = \dot{\rho}_{V,2} = 0$. This is done under the assumption that the energy difference between the real and virtual subspaces is much larger than the coupling rate, i.e., $\Delta_V \gg \Omega$. Thus, by substituting the virtual coherence terms by their steady-state values, the system gets described by the following differential equations:

$$\dot{\rho}_{1,2} \approx \left(-\frac{\Gamma}{2} + \frac{\Gamma\Omega^2}{(i\Gamma - 2\Delta_V)\Delta_V}\right)\rho_{1,2}(t) - \frac{i\Omega^2}{\Delta_V} + \left(-\frac{2\Omega^2}{\Gamma + 2i\Delta_V} + \frac{i\Omega^2}{\Delta_V}\right)\rho_{2,2}(t) + \left(\frac{2\Omega^2}{\Gamma + 2i\Delta_V} + \frac{2i\Omega^2}{\Delta_V}\right)\rho_{V,V}(t), \tag{A1a}$$

$$\dot{\rho}_{2,2} \approx \left(-\Gamma - \frac{4\Gamma\Omega^2}{\Gamma^2 + 4\Delta_V^2}\right)\rho_{2,2}(t) - \frac{2\Omega^2}{\Gamma + 2i\Delta_V}\rho_{1,2}(t) - \frac{2\Omega^2}{\Gamma - 2i\Delta_V}\rho_{2,1}(t) + \frac{4\Gamma\Omega^2}{\Gamma^2 + 4\Delta_V^2}\rho_{V,V}(t). \tag{A1b}$$

In the limit $\Delta_V \gg \Gamma$, we can simplify them and obtain a more familiar set of equations,

$$\dot{\rho}_{1,2} \approx -\frac{\Gamma}{2}\rho_{1,2}(t) - i\Omega_{2p}[1 - 2\rho_{2,2}(t)] + i\Omega_{2p}\rho_{V,V}(t), \tag{A2a}$$

$$\dot{\rho}_{2,2} \approx -\Gamma\rho_{2,2}(t) - 2\Omega_{2p}\mathrm{Im}[\rho_{1,2}(t)] + \frac{\Gamma}{\Delta_V}\Omega_{2p}\rho_{V,V}(t). \tag{A2b}$$

These equations resemble those that would correspond to a two-level system driven with a Rabi frequency, $\Omega_{2p} \equiv \Omega^2/\Delta_V$, and a decay rate Γ. The only addition is an extra term related to the virtual population, $\rho_{V,V}$. However, this term evolves in a much slower timescale than $\rho_{1,2}$ and $\rho_{2,2}$, so in these equations it can be treated as a time-independent parameter with a fixed value. At the beginning of the evolution, we may set $\rho_{V,V} = 0$. The time-dependent analytical solutions of these equations are well known and can be found in any quantum optics textbook,

$$\rho_{2,2}(t) \approx \frac{4\Omega_{2p}^2}{\Gamma^2 + 8\Omega_{2p}^2}\left[1 - e^{-3\Gamma t/4}\left(\cosh(\kappa t) + \frac{3\Gamma}{4\kappa}\sinh(\kappa t)\right)\right], \tag{A3a}$$

$$\rho_{1,2}(t) \approx \frac{-2i\Omega_{2p}\Gamma}{\Gamma^2 + 8\Omega_{2p}^2}\left[1 - e^{-3\Gamma t/4}\left(\cosh(\kappa t) + \left(\frac{\kappa}{\Gamma} + \frac{3\Gamma}{16\kappa}\right)\sinh(\kappa t)\right)\right], \tag{A3b}$$

where $\kappa \equiv \frac{1}{2}\sqrt{\frac{\Gamma^2}{4} - 16\Omega_{2p}^2}$. One can clearly see that, for these equations, the relaxation time towards a stationary state occurs in a timescale $\sim 1/\Gamma$.

2. Second adiabatic elimination

In much longer timescales than $1/\Gamma$, $\rho_{2,2}$ and $\rho_{1,2}$ can be considered as "fast" variables, since they relax to a steady state in a very short time. This allows us to perform a second adiabatic elimination: from Eqs. (A2), it is clear that, if we assume that $\rho_{V,V}$ will be virtually unchanged in a timescale $\sim 1/\Gamma$, we could take it as a time-independent parameter and obtain a stationary solution for $\rho_{2,2}$ and $\rho_{1,2}$ that is dependent on the fixed value of $\rho_{V,V}$. This quasisteady state will adiabatically follow any slow change of $\rho_{V,V}$ taking place in a much longer characteristic timescale. The expression of this $\rho_{V,V}$-dependent steady state can be obtained by solving a linear system of equations of the form $\hat{M}\cdot\vec{\rho} + \vec{b} = 0$ for the vector $\vec{\rho} = \{\rho_{2,2}^{SS}, \rho_{2,1}^{SS}, \rho_{1,2}^{SS}\}$, where $\hat{M}$ and $\vec{b}$ are given by

$$\hat{M} = \begin{bmatrix} -\Gamma\left(1 + \frac{4\Omega^2}{\Gamma^2+4\Delta_V^2}\right) & -\frac{2\Omega^2}{\Gamma-2i\Delta_V} & -\frac{2\Omega^2}{\Gamma+2i\Delta_V} \\ -\frac{2\Omega^2}{\Gamma-2i\Delta_V} - i\Omega_{2p} & -\Gamma\left(\frac{1}{2} - \frac{i\Omega_{2p}}{\Gamma-2i\Delta_V}\right) & 0 \\ -\frac{2\Omega^2}{\Gamma+2i\Delta_V} + i\Omega_{2p} & 0 & -\Gamma\left(\frac{1}{2} - \frac{\Gamma\Omega_{2p}}{i\Gamma-2\Delta_V}\right) \end{bmatrix}, \tag{A4}$$

$$\vec{b} = \begin{pmatrix} \frac{4\Gamma\Omega^2}{\Gamma^2+4\Delta_V^2} \\ \frac{2\Omega^2}{\Gamma-2i\Delta_V} - 2i\Omega_{2p} \\ \frac{2\Omega^2}{\Gamma+2i\Delta_V} + 2i\Omega_{2p} \end{pmatrix}\rho_{V,V}(t) + \begin{pmatrix} 0 \\ i\Omega_{2p} \\ -i\Omega_{2p} \end{pmatrix}. \tag{A5}$$

By solving this linear system, we obtain a set of equations for the quasistationary values of $\rho_{2,2}$ and $\rho_{1,2}$ that depend on the population of the virtual state at any given time,

$$\begin{aligned}\rho_{2,2}^{\mathrm{SS}}[\rho_{V,V}(t)] = &\frac{16\Omega^4\left(\Delta_V^2+\Omega^2\right)}{\Gamma^4\Delta_V^2+32\Omega^2\left(\Delta_V^2+\Omega^2\right)+4\Gamma^2\left(\Delta_V^4+3\Delta_V^2\Omega^2+\Omega^4\right)}\\ &+\frac{4\left[\Gamma^2\Delta_V^2\Omega^2-4\Omega^4\left(\Delta_V^2+\Omega^2\right)\right]}{\Gamma^4\Delta_V^2+32\Omega^2\left(\Delta_V^2+\Omega^2\right)+4\Gamma^2\left(\Delta_V^4+3\Delta_V^2\Omega^2+\Omega^4\right)}\rho_{V,V}(t),\end{aligned} \tag{A6}$$

$$\begin{aligned}\rho_{1,2}^{\mathrm{SS}}[\rho_{V,V}(t)] = &\frac{2\Omega^2\left[-i\Gamma\Delta_V\left(\Gamma^2+4\Delta_V^2\right)-2\Gamma\Omega^2(\Gamma+4i\Delta_V)-8\Omega^4\right]}{4\Gamma^2\left(3\Delta_V^2\Omega^2+\Delta_V^4+\Omega^4\right)+\Gamma^4\Delta_V^2+32\Omega^4\left(\Delta_V^2+\Omega^2\right)}\\ &+\frac{4\Omega^2[2\Gamma\Omega^2(\Gamma+4i\Delta_V)+\Gamma\Delta_V(\Gamma+i\Delta_V)(2\Delta+i\Gamma)+12\Omega^4]}{4\Gamma^2\left(3\Delta_V^2\Omega^2+\Delta_V^4+\Omega^4\right)+\Gamma^4\Delta_V^2+32\Omega^4\left(\Delta_V^2+\Omega^2\right)}\rho_{V,V}(t).\end{aligned} \tag{A7}$$

Notice that after the first adiabatic elimination, the differential equation that governs the dynamics of $\rho_{V,V}$ became

$$\dot{\rho}_{V,V}(t) \approx -\frac{4\Gamma\Omega^2}{\Gamma^2+4\Delta_V^2}\rho_{V,V}+\frac{\Omega_{2\mathrm{p}}\Gamma(i\Gamma+2\Delta_V)}{\Gamma^2+4\Delta_V^2}\rho_{1,2}+\frac{\Omega_{2\mathrm{p}}\Gamma(-i\Gamma+2\Delta_V)}{\Gamma^2+4\Delta_V^2}\rho_{2,1}+\frac{4\Gamma}{\Gamma^2+4\Delta^2}\rho_{2,2}. \tag{A8}$$

We can then substitute the pseudostationary values of $\rho_{1,2}$ and $\rho_{2,2}$ into this equation, and we obtain a differential equation for $\rho_{V,V}(t)$ that is a function of itself, i.e., $\dot{\rho}_{V,V}(t) = f[\rho_{V,V}(t); \rho_{1,2}^{\mathrm{SS}}[\rho_{V,V}(t)]; \rho_{2,2}^{\mathrm{SS}}[\rho_{V,V}(t)]]$. Namely, the differential equation for the virtual-state population becomes

$$\dot{\rho}_{V,V}(t) = \frac{4\Gamma\Omega^4(\Gamma^2+4\Omega^2)}{\chi}-\frac{4\left[12\Gamma\Omega^6+\Gamma^3\Omega^2\left(\Delta_V^2+2\Omega^2\right)\right]}{\chi}\rho_{V,V}(t) \tag{A9}$$

with

$$\chi \equiv \Gamma^4\Delta_V^2+32\Omega^2\left(\Delta_V^2+\Omega^2\right)+4\Gamma^2\left(\Delta_V^4+3\Delta_V^2\Omega^2+\Omega^4\right). \tag{A10}$$

Solving this equation, we obtain an analytical expression for the evolution of $\rho_{V,V}(t)$,

$$\rho_{V,V}(t) = \rho_{V,V}^{\mathrm{SS}}(1-e^{-\Gamma_c t}), \tag{A11}$$

where $\rho_{V,V}^{\mathrm{SS}}$ stands for the steady-state value,

$$\rho_{V,V}^{\mathrm{SS}} = \frac{\Omega^2(\Gamma^2+4\Omega^2)}{\Gamma^2\left(\Delta_V^2+2\Omega^2\right)+12\Omega^4}, \tag{A12}$$

and Γ_c stands for the relaxation rate,

$$\Gamma_c = \frac{4\left[12\Gamma\Omega^6+\Gamma^3\Omega^2\left(\Delta_V^2+2\Omega^2\right)\right]}{\chi}, \tag{A13}$$

which gives us an analytical estimation of the Liouvillian gap. We can reduce this equation under the assumption $\Delta_V \gg \Omega, \Gamma$ and the effective strong-coupling regime $\Omega_{2\mathrm{p}} \gg \Gamma$. In this situation, the relaxation rate reduces to

$$\Gamma_c \approx \frac{3\Gamma\Omega^2}{2\Delta_V^2}, \tag{A14}$$

which is the expression shown in the main text.

3. Summary of analytic expressions for the time-dependent density matrix elements

Once we know the analytic expression for the time-dependent virtual-state population, the remaining equations are easily computed:

$$\rho_{V,V}(t) \approx \rho_{V,V}^{\mathrm{SS}}[1-e^{-\Gamma_c t}], \tag{A15a}$$

$$\rho_{2,2}(t) \approx \rho_{2,2}^{\mathrm{SS}}\left[1+\frac{4\Omega^4\left(\Gamma^2+4\Delta_V^2\right)-\Gamma^4\Delta_V^2+16\Omega^6}{4\Gamma^2\left(3\Delta_V^2\Omega^2+\Delta_V^4+\Omega^4\right)+\Gamma^4\Delta_V^2+32\Omega^4\left(\Delta_V^2+\Omega^2\right)}e^{-\Gamma_c t}\right], \tag{A15b}$$

$$\rho_{1,2}(t) \approx \rho_{1,2}^{\mathrm{SS}}\left[1-\frac{2i\Omega^2(\Gamma^2+4\Omega^2)[2\Gamma\Omega^2(\Gamma+4i\Delta_V)+\Gamma\Delta_V(\Gamma+i\Delta_V)(2\Delta_V+i\Gamma)+12\Omega^4]}{\Gamma\Delta_V\left[4\Gamma^2\left(3\Delta_V^2\Omega^2+\Delta_V^4+\Omega^4\right)+\Gamma^4\Delta_V^2+32\Omega^4\left(\Delta_V^2+\Omega^2\right)\right]}e^{-\Gamma_c t}\right], \tag{A15c}$$

$$\rho_{1,V}(t) \approx \rho_{1,V}^{\mathrm{SS}}\left[1+\frac{2\Omega^2(\Gamma^2+4\Omega^2)\left[-2i\Gamma\Omega^2\left(\Gamma^2+6i\Gamma\Delta_V+2\Delta_V^2\right)+\Gamma^2\Delta_V\left(\Gamma^2+4\Delta_V^2\right)+8\Omega^4(3\Delta_V-2i\Gamma)\right]}{\Gamma(\Gamma\Delta_V-2i\Omega^2)\left[4\Gamma^2\left(3\Delta_V^2\Omega^2+\Delta_V^4+\Omega^4\right)+\Gamma^4\Delta_V^2+32\Omega^4\left(\Delta_V^2+\Omega^2\right)\right]}e^{-\Gamma_c t}\right], \tag{A15d}$$

$$\rho_{2,V}(t) \approx \rho_{2,V}^{\mathrm{SS}}\left[1-\frac{(\Gamma^2+4\Omega^2)\left[\Gamma^2\Delta_V^2(\Gamma+2i\Delta_V)-4\Omega^4(\Gamma-6i\Delta_V)+4i\Gamma\Delta_V\Omega^2(\Gamma+i\Delta_V)\right]}{4\Gamma^3\left(3\Delta_V^2\Omega^2+\Delta_V^4+\Omega^4\right)+\Gamma^5\Delta_V^2+32\Gamma\Omega^4\left(\Delta_V^2+\Omega^2\right)}e^{-\Gamma_c t}\right], \tag{A15e}$$

where $\rho_{i,j}^{\mathrm{SS}}$ $(i,j=1,2,V)$ are the steady-state density matrix elements,

$$\rho_{2,2}^{\mathrm{SS}} = \frac{4\Omega^4}{\Gamma^2\left(\Delta_V^2+2\Omega^2\right)+12\Omega^4}, \tag{A16a}$$

$$\rho_{1,2}^{\mathrm{SS}} = -\frac{2i\Gamma\Delta_V\Omega^2}{\Gamma^2\left(\Delta_V^2+2\Omega^2\right)+12\Omega^4}, \tag{A16b}$$

$$\rho_{1,V}^{\mathrm{SS}} = \frac{\Gamma\Omega(-\Gamma\Delta_V+2i\Omega^2)}{\Gamma^2\left(\Delta_V^2+2\Omega^2\right)+12\Omega^4}, \tag{A16c}$$

$$\rho_{2,V}^{\mathrm{SS}} = -\frac{2i\Gamma\Omega^3}{\Gamma^2\left(\Delta_V^2+2\Omega^2\right)+12\Omega^4}. \tag{A16d}$$

The stationary values of $\rho_{2,2}$ and $\rho_{1,2}$ reached in the metastable regime are the long-time limit of Eqs. (A3a) and (A3b),

$$\rho_{2,2}^{M} = \frac{4\Omega_{2\mathrm{p}}^2}{\Gamma^2+8\Omega_{2\mathrm{p}}^2}, \quad \rho_{1,2}^{M} = \frac{-2i\Gamma\Omega_{2\mathrm{p}}}{\Gamma^2+8\Omega_{2\mathrm{p}}^2}. \tag{A17}$$

APPENDIX B: VALIDITY OF THE DIFFERENT APPROXIMATIONS OF THE LIOUVILLIAN GAP Γ_c

In this Appendix, we analyze in further detail the validity of the estimations of Γ_c via the HAE under different approximations. In Fig. 2(a), the general expression for Γ_c in Eq. (A14) was used in order to compute the analytical curves for the population dynamics, instead of the reduced expression shown in the main text, Eq. (10). It is therefore interesting to offer a comparison between both expressions and clarify their regimes of validity, particularly when the condition $\Omega_{2\mathrm{p}} \gg \Gamma$—assumed for the derivation of the simplified expression for Γ_c—no longer holds. We remind the reader that Γ_c is the relaxation rate towards the steady state, and therefore it is expected to correspond to the Liouvillian gap.

Figure 5(a) shows an exact calculation of the Liouvillian gap versus Γ and Ω, compared to the estimations of Γ_c given by Eq. (A14) (full expression) and Eq. (10) (simplified expression). This calculation confirms that both expressions provide a good approximation of the Liouvillian gap when the assumption $\Omega_{2\mathrm{p}} \gg \Gamma$ holds, as can be seen in the lower-right section of Fig. 5(a). For $\Omega_{2\mathrm{p}} < \Gamma$, the simplified expression of Γ_c slightly deviates from the exact value, although the difference is not dramatic. The eigenvalue crossing that occurs when $\Gamma \gg \Omega_{2\mathrm{p}}$ [see Fig. 2(d)] manifests as a kink in the Liouvillian gap, which is not captured by any of the analytical expressions obtained from the HAE (this is, however, an overdamped regime not expected to yield any particularly interesting dynamics). We note that, even in the regime $\Omega_{2\mathrm{p}} < \Gamma$, the simplified expressions of Γ_c still provide a very good approximation of the timescale of relaxation towards the steady state, as shown in the example of Fig. 5(b).

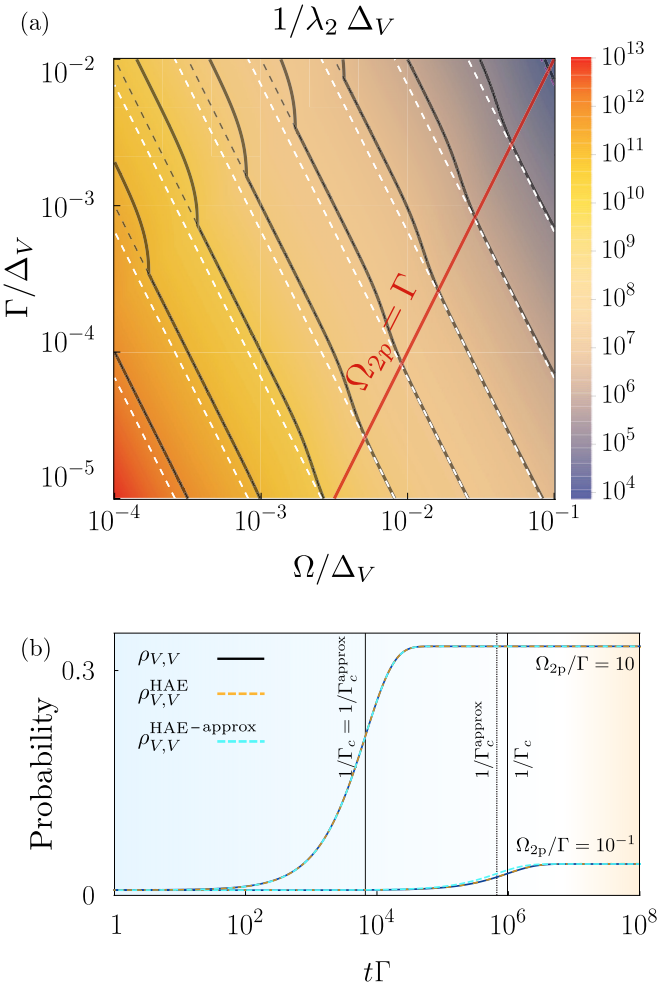

FIG. 5. (a) Liouvillian gap in terms of Ω/Δ_v and Γ/Δ_v. Solid black lines are exact computations, dashed black lines are analytical predictions from the relaxation rate, Eq. (A13), and dashed white lines are analytical predictions from the approximated relaxation rate, Eq. (10). The solid red line divides the figure into the two-photon weak driving regime (left) and the two-photon strong driving regime (right). (b) Dynamics of the virtual population at two different regimes: strong driving $\Omega_{2\mathrm{p}}/\Gamma = 10$ and weak driving $\Omega_{2\mathrm{p}}/\Gamma = 10^{-1}$. Solid lines correspond to numerical calculations, dashed lines are analytical predictions from the hierarchical adiabatic elimination considering the complete relaxation rate, indicated in the figure as $\rho_{V,V}^{\mathrm{HAE}}$, and the approximated relaxation rate, indicated in the figure as $\rho_{V,V}^{\mathrm{HAE\text{-}approx}}$. Parameters: (b) $\Gamma/\Delta_V = 10^{-5}$; strong driving, $\Omega/\Delta_V = 10^{-2}$; weak driving, $\Omega/\Delta_V = 10^{-3}$.

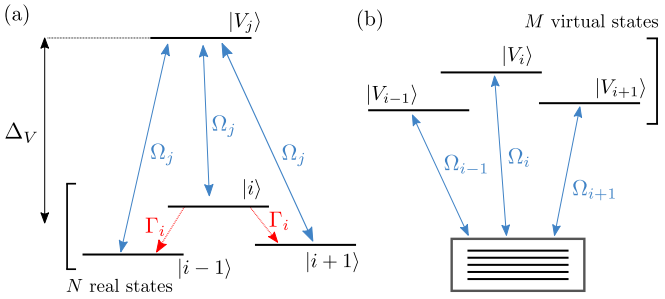

FIG. 6. (a) N real states in a quasiresonant energy manifold interacting with a single virtual state. (b) N real states in a quasiresonant energy manifold interacting with M virtual states.

APPENDIX C: APPLICATION OF THE HIERARCHICAL ADIABATIC ELIMINATION TO ARBITRARY SYSTEMS: COMPUTATIONAL COST

In this work, the hierarchical adiabatic elimination method has been applied to two specific systems with a small Hilbert space. Here, we discuss the implications of applying this technique in systems of arbitrary size, focusing in particular on the computational cost associated with the technique.

Let us assume that we aim to describe a general system with N quasiresonant real states and M off-resonant virtual states, as is sketched in Fig. 6. These states span a basis $\{|i\rangle\}$ with $i = 1, \ldots, N+M$, where we assume the indexes are organized such that the first N states are the real states, and the last M states are the virtual ones. To make explicit that one index corresponds to a virtual state, we will use the notation $|V_j\rangle \equiv |N+j\rangle$, with $j = 1, \ldots, M$.

Formally, computation of the dynamics would imply solving $(N+M)^2 - 1$ coupled differential equations for the all density matrix elements $\rho_{i,j} = \langle i|\hat{\rho}|j\rangle$, excluding one of the diagonal elements that can be eliminated by applying the condition $\mathrm{Tr}[\hat{\rho}] = 1$. Let us discuss the different steps involved in solving the dynamics of such a system by means of the HAE.

1. First adiabatic elimination

At the first stage of the HAE, we set the derivative of real-virtual coherences to zero,

$$\dot{\rho}_{i,V_j} = 0, \tag{C1}$$

where $i = 1, \ldots, N$ and $j = 1, \ldots, M$. In total, there are a number $N_c = 2M \times N$ of these terms. The first adiabatic elimination consists of solving the N_c equations (C1) for these N_c variables.

The solutions are expressed in terms of the remaining $N^2 + M^2 - 1$ variables, corresponding to all the populations and coherences within the real and virtual subspaces, respectively, reduced by 1 due to the population normalization.

2. Second adiabatic elimination

The second step of the adiabatic elimination corresponds to solving for the steady-state dynamics within the real sector, leaving the M^2 variables of the virtual sector as fixed, time-independent parameters. Therefore, one has to solve a linear system of equations of the form

$$\hat{W} \cdot \vec{\rho} + \vec{b} = 0, \tag{C2}$$

where $\hat{W}$ is a matrix of dimension $(N^2-1) \times (N^2-1)$, and $\vec{\rho}$, $\vec{b}$ are vectors of dimension (N^2-1). Here, $\vec{\rho}$ corresponds to the flattened density matrix of the real sector, i.e.,

$$\vec{\rho} = (\rho_{1,1},\ \rho_{1,2}, \ldots,\ \rho_{N,N-1})^{\mathrm{T}}, \tag{C3}$$

where element $\rho_{N,N}$ is not included since it is removed by applying the population normalization condition. Similarly,

$$\vec{b} = \hat{\Lambda}\vec{\rho}_V + \vec{\mu}, \tag{C4}$$

where $\hat{\Lambda}$ is an $(N^2-1) \times M^2$ matrix, $\vec{\rho}_V$ is the vectorial representation of size M^2 of the density matrix of the virtual sector, and $\vec{\mu}$ is a vector of dimension (N^2-1). The stationary solution of this coupled system will take the functional form

$$\vec{\rho}_{\mathrm{SS}} = \vec{\rho}_{\mathrm{SS}}[\vec{\rho}_V(t)]. \tag{C5}$$

The solution of this linear system of $N^2 - 1$ equations allows us to write the set of differential equations that governs the dynamics of $\vec{\rho}_V(t)$ with the following functional structure:

$$\dot{\vec{\rho}}_V = f[\vec{\rho}_V, \vec{\rho}_{\mathrm{SS}}[\vec{\rho}_V(t)]]. \tag{C6}$$

This can be written as a standard matrix differential equation of the form $\dot{\vec{\rho}}_V = \hat{A} \cdot \vec{\rho}_V(t) + \vec{B}$, where $\hat{A}$ is a matrix of dimension $M^2 \times M^2$, and $\vec{B}$ is a vector of dimension M^2.

3. Summary

In summary, given N real states and M virtual states, the method of HAE allows us to write an effective, linear differential equation for the M^2 slow degrees of freedom (the virtual sector) after performing the following calculations:

(i) Solving a linear system of $2M \times N$ equations.

(ii) Solving a second linear system of $N^2 - 1$ equations.

The availability of manageable closed-form expressions for the final differential equation and the associated eigenvalues will depend strongly on the complexity of the initial problem and will not always be guaranteed. However, let us stress that, even in the case in which closed-form expressions are difficult to obtain, the HAE can prove to be computationally useful, since it would allow us to reduce the computational cost of numerically computing the Liouvillian gap from diagonalizing an $(N+M)^2 \times (N+M)^2$ matrix to diagonalizing an $M^2 \times M^2$ matrix.

[1] C. Cohen-Tannoudji, J. Dupont-Roc, and G. Grynberg, *Photons and Atoms* (Wiley, New York, 1989).

[2] C. Cohen-Tannoudji, J. Dupont-Roc, and G. Grynberg, *Atom-Photon Interactions* (Wiley, New York, 1998).

[3] J. J. Sakurai and J. Napolitano, *Modern Quantum Mechanics* (Cambridge University Press, Cambridge, 2017).

[4] L. H. Ryder, *Quantum Field Theory* (Cambridge University Press, Cambridge, 1996).

[5] U. Gaubatz, P. Rudecki, S. Schiemann, and K. Bergmann, Population transfer between molecular vibrational levels by stimulated Raman scattering with partially overlapping laser fields. A new concept and experimental results, J. Chem. Phys. **92**, 5363 (1990).

[6] K. Bergmann, H. Theuer, and B. W. Shore, Coherent population transfer among quantum states of atoms and molecules, Rev. Mod. Phys. **70**, 1003 (1998).

[7] N. Lütkenhaus, J. I. Cirac, and P. Zoller, Mimicking a squeezed-bath interaction: Quantum-reservoir engineering with atoms, Phys. Rev. A **57**, 548 (1998).

[8] P. Warszawski and H. M. Wiseman, Adiabatic elimination in compound quantum systems with feedback, Phys. Rev. A **63**, 013803 (2000).

[9] E. Brion, L. H. Pedersen, and K. Mølmer, Adiabatic elimination in a lambda system, J. Phys. A **40**, 1033 (2007).

[10] F. Dimer, B. Estienne, A. S. Parkins, and H. J. Carmichael, Proposed realization of the Dicke-model quantum phase transition in an optical cavity QED system, Phys. Rev. A **75**, 013804 (2007).

[11] D. Burgarth, P. Facchi, H. Nakazato, S. Pascazio, and K. Yuasa, Generalized adiabatic theorem and strong-coupling limits, Quantum **3**, 152 (2019).

[12] O. Gamel and D. F. V. James, Time-averaged quantum dynamics and the validity of the effective Hamiltonian model, Phys. Rev. A **82**, 052106 (2010).

[13] F. Damanet, A. J. Daley, and J. Keeling, Atom-only descriptions of the driven-dissipative Dicke model, Phys. Rev. A **99**, 033845 (2019).

[14] B. Kaufman, T. Rozgonyi, P. Marquetand, and T. Weinacht, Adiabatic elimination in strong-field light-matter coupling, Phys. Rev. A **102**, 063117 (2020).

[15] D. Burgarth, P. Facchi, H. Nakazato, S. Pascazio, and K. Yuasa, Eternal adiabaticity in quantum evolution, Phys. Rev. A **103**, 032214 (2021).

[16] L. Garziano, R. Stassi, V. Macrì, A. F. Kockum, S. Savasta, and F. Nori, Multiphoton quantum Rabi oscillations in ultrastrong cavity QED, Phys. Rev. A **92**, 063830 (2015).

[17] L. Garziano, V. Macrì, R. Stassi, O. Di Stefano, F. Nori, and S. Savasta, One Photon Can Simultaneously Excite Two or More Atoms, Phys. Rev. Lett. **117**, 043601 (2016).

[18] R. Stassi, V. Macrì, A. F. Kockum, O. Di Stefano, A. Miranowicz, S. Savasta, and F. Nori, Quantum nonlinear optics without photons, Phys. Rev. A **96**, 023818 (2017).

[19] D. Comparat, General conditions for quantum adiabatic evolution, Phys. Rev. A **80**, 012106 (2009).

[20] M. Mirrahimi and P. Rouchon, Singular perturbations and Lindblad-Kossakowski differential equations, IEEE Trans. Autom. Control **54**, 1325 (2009).

[21] V. Paulisch, H. Rui, H. K. Ng, and B.-G. Englert, Beyond adiabatic elimination: A hierarchy of approximations for multiphoton processes, Eur. Phys. J. Plus **129**, 12 (2014).

[22] A. C. Santos and M. S. Sarandy, Generalized transitionless quantum driving for open quantum systems, Phys. Rev. A **104**, 062421 (2021).

[23] F. Reiter and A. S. Sørensen, Effective operator formalism for open quantum systems, Phys. Rev. A **85**, 032111 (2012).

[24] R. Azouit, A. Sarlette, and P. Rouchon, Adiabatic elimination for open quantum systems with effective Lindblad master equations, in *2016 IEEE 55th Conference on Decision and Control (CDC)* (IEEE, Piscataway, NJ, 2016), pp. 4559–4565.

[25] D. Finkelstein-Shapiro, D. Viennot, I. Saideh, T. Hansen, T. Pullerits, and A. Keller, Adiabatic elimination and subspace evolution of open quantum systems, Phys. Rev. A **101**, 042102 (2020).

[26] M. B. Plenio, S. F. Huelga, A. Beige, and P. L. Knight, Cavity-loss-induced generation of entangled atoms, Phys. Rev. A **59**, 2468 (1999).

[27] S. Diehl, A. Micheli, A. Kantian, B. Kraus, H. P. Büchler, and P. Zoller, Quantum states and phases in driven open quantum systems with cold atoms, Nat. Phys. **4**, 878 (2008).

[28] F. Verstraete, M. M. Wolf, and J. Ignacio Cirac, Quantum computation and quantum-state engineering driven by dissipation, Nat. Phys. **5**, 633 (2009).

[29] G. Vacanti and A. Beige, Cooling atoms into entangled states, New J. Phys. **11**, 083008 (2009).

[30] J. Busch and A. Beige, Protecting subspaces by acting on the outside, J. Phys.: Conf. Ser. **254**, 012009 (2010).

[31] M. J. Kastoryano, F. Reiter, and A. S. Sørensen, Dissipative Preparation of Entanglement in Optical Cavities, Phys. Rev. Lett. **106**, 090502 (2011).

[32] J. Busch, S. De, S. S. Ivanov, B. T. Torosov, T. P. Spiller, and A. Beige, Cooling atom-cavity systems into entangled states, Phys. Rev. A **84**, 022316 (2011).

[33] Y. Lin, J. P. Gaebler, F. Reiter, T. R. Tan, R. Bowler, A. S. Sørensen, D. Leibfried, and D. J. Wineland, Dissipative production of a maximally entangled steady state of two quantum bits, Nature (London) **504**, 415 (2013).

[34] R. E. Evans, M. K. Bhaskar, D. D. Sukachev, C. T. Nguyen, A. Sipahigil, M. J. Burek, B. Machielse, G. H. Zhang, A. S. Zibrov, E. Bielejec, H. Park, M. Lončar, and M. D. Lukin, Photon-mediated interactions between quantum emitters in a diamond nanocavity, Science **362**, 662 (2018).

[35] D. E. Chang, J. S. Douglas, A. González-Tudela, C.-L. Hung, and H. J. Kimble, Colloquium: Quantum matter built from nanoscopic lattices of atoms and photons, Rev. Mod. Phys. **90**, 031002 (2018).

[36] K. Macieszczak, M. Gu, I. Lesanovsky, and J. P. Garrahan, Towards a Theory of Metastability in Open Quantum Dynamics, Phys. Rev. Lett. **116**, 240404 (2016).

[37] K. Macieszczak, D. C. Rose, I. Lesanovsky, and J. P. Garrahan, Theory of classical metastability in open quantum systems, Phys. Rev. Research **3**, 033047 (2021).

[38] M. B. Plenio and P. L. Knight, The quantum-jump approach to dissipative dynamics in quantum optics, Rev. Mod. Phys. **70**, 101 (1998).

[39] T. A. Brun, A simple model of quantum trajectories, Am. J. Phys. **70**, 719 (2002).

[40] C. Gerry and P. Knight, *Introductory Quantum Optics* (Cambridge University Press, Cambridge, 2004).

[41] T. Ramos, H. Pichler, A. J. Daley, and P. Zoller, Quantum Spin Dimers from Chiral Dissipation in Cold-Atom Chains, Phys. Rev. Lett. **113**, 237203 (2014).

[42] H. Pichler, T. Ramos, A. J. Daley, and P. Zoller, Quantum optics of chiral spin networks, Phys. Rev. A **91**, 042116 (2015).

[43] G. V. Varada and G. S. Agarwal, Two-photon resonance induced by the dipole-dipole interaction, Phys. Rev. A **45**, 6721 (1992).

[44] C. Hettich, C. Schmitt, J. Zitzmann, S. Kühn, I. Gerhardt, and V. Sandoghdar, Nanometer resolution and coherent optical dipole coupling of two individual molecules. Science **298**, 385 (2002).

[45] H. R. Haakh and D. Martín-Cano, Squeezed light from entangled nonidentical emitters via nanophotonic environments, ACS Photon. **2**, 1686 (2015).

[46] A. Vivas-Viaña and C. Sánchez Muñoz, Two-photon resonance fluorescence of two interacting nonidentical quantum emitters, Phys. Rev. Research **3**, 033136 (2021).

[47] E. del Valle, S. Zippilli, F. P. Laussy, A. Gonzalez-Tudela, G. Morigi, and C. Tejedor, Two-photon lasing by a single quantum dot in a high-Q microcavity, Phys. Rev. B **81**, 035302 (2010).

[48] Y. Ota, S. Iwamoto, N. Kumagai, and Y. Arakawa, Spontaneous Two-Photon Emission from a Single Quantum Dot, Phys. Rev. Lett. **107**, 233602 (2011).

[49] H.-P. Breuer and F. Petruccione, *The Theory of Open Quantum Systems* (Oxford University Press, Oxford, 2007).

[50] E. M. Kessler, G. Giedke, A. Imamoglu, S. F. Yelin, M. D. Lukin, and J. I. Cirac, Dissipative phase transition in a central spin system, Phys. Rev. A **86**, 012116 (2012).

[51] H. Haken, *Synergetics* (Springer, Berlin, 2004).

[52] S. Haroche and J.-M. Raimond, *Exploring the Quantum: Atoms, Cavities, and Photons* (Oxford University Press, Oxford, 2006).

[53] W. K. Wootters, Entanglement of Formation of an Arbitrary State of Two Qubits, Phys. Rev. Lett. **80**, 2245 (1998).

[54] W. K. Wootters, Entanglement of formation and concurrence, Quantum Inf. Comput. **1**, 27 (2001).

[55] M. B. Plenio and S. Virmani, An introduction to entanglement measures, Quantum Inf. Comput. **7**, 1 (2007).

[56] R. Horodecki, P. Horodecki, M. Horodecki, and K. Horodecki, Quantum entanglement, Rev. Mod. Phys. **81**, 865 (2009).

[57] A. Gonzalez-Tudela, D. Martin-Cano, E. Moreno, L. Martin-Moreno, C. Tejedor, and F. J. Garcia-Vidal, Entanglement of Two Qubits Mediated by One-Dimensional Plasmonic Waveguides, Phys. Rev. Lett. **106**, 020501 (2011).